How alpha rhythm spatiotemporally acts upon the thalamus-default mode circuit in idiopathic generalized epilepsy

Yun Qin, Nan Zhang, Yan Chen, Yue Tan, Li Dong, Peng Xu, Daqing Guo, Tao Zhang, Dezhong Yao, Cheng Luo*

***Abstract*— *Goal:* Idiopathic generalized epilepsy (IGE) represents generalized spike-wave discharges (GSWD) and distributed changes in thalamocortical circuit. The purpose of this study is to investigate how the ongoing alpha oscillation acts upon the local temporal dynamics and spatial hyperconnectivity in epilepsy. *Methods:* We evaluated the spatiotemporal regulation of alpha oscillations in epileptic state based on simultaneous EEG-fMRI recordings in 45 IGE patients. The alpha-BOLD temporal consistency, as well as the effect of alpha power windows on dynamic functional connectivity strength (dFCS) was analyzed. Then, stable synchronization networks during GSWD were constructed, and the spatial covariation with alpha-based network integration was investigated. *Results:* Increased temporal covariation was demonstrated between alpha power and BOLD fluctuations in thalamus and distributed cortical regions in IGE. High alpha power had inhibition effect on dFCS in healthy controls, while in epilepsy, high alpha windows arose along with the enhancement of dFCS in thalamus, caudate and some default mode network (DMN) regions. Moreover, synchronization networks in GSWD-before, GSWD-onset and GSWD-after stages were constructed, and the connectivity strength in prominent hub nodes (precuneus, thalamus) was associated with the spatially disturbed alpha-based network integration. *Conclusion:* The results indicated spatiotemporal regulation of alpha in epilepsy by means of the increased power and decreased coherence communication. It provided links between alpha rhythm and the altered temporal dynamics, as well as the hyperconnectivity in thalamus-default mode circuit. *Significance:* The combination between neural oscillations and epileptic representations may be of clinical importance in terms of seizure prediction and non-invasive interventions.**

***Index Terms*—Alpha oscillation, spatiotemporal regulation, simultaneous EEG-fMRI, dynamic functional connectivity, epilepsy.**

I. Introduction

IDIOPATHIC generalized epilepsy (IGE) forms a group of epileptic syndromes manifesting as absence seizures, tonic-clonic seizures, myoclonic jerks. The epilepsy brains have numerous additional features to their dynamic repertoire, including the temporal paroxysmal occurrence of discharges, as well as the altered network connectomics [1-3]. EEG recordings have showed stereotyped 3-6 Hz generalized spike-wave discharges (GSWD) or polyspike-wave activity with frontocentral predominance in IGE [4, 5]. Current concepts based on animal models postulated that GSWD bursts originated from the interaction between thalamus and cortices [6-8]. Moreover, widespread synchronization was revealed a few hundred milliseconds before GSWD [9], while recent fMRI studies found distributed activity in thalamocortical circuit preceding GSWD underlying the transition from normal neuronal activity to a short-lasting generalized hypersynchrony [10]. Although the role of thalamus and cortices during GSWD has been extensively demonstrated, pathophysiological substrate of GSWD remains enigmatic, and in what ways do the cortical and subcortical structures gate the discharges remains unclear.

Healthy brains have their own optimal level and reflect specific EEG oscillation and network variables subserving brain stability and optimal network operation [11]. Ongoing oscillations were found contributing to the temporal modulation of information processing and reflecting cognitive performance [12, 13]. Altered oscillation regulations were suggested relating to the diffuse and hypersynchronous state in patients with epilepsy [14]. However, how the ongoing oscillations act upon the temporal dynamics and spatial connectivity in epilepsy state has not been yet demonstrated. Especially, we hypothesize that

This work was supported by the grant from the National Key R&D Program of China (No. 2018YFA0701400) and grants from the National Nature Science Foundation of China 61933003, 81771822, 81701778, 31771149, and 81861128001, and in part by Sichuan Science and Technology Program 2018JZ0073, 2019YJ0179, and the CAMS Innovation Fund for Medical Sciences（CIFMS）2019-I2M-5-039. (Corresponding author: Cheng Luo.)

Y. Qin, N. Zhang, Y. Chen, Y. Tan, L. Dong, P. Xu, D. Guo and T. Zhang are with the Clinical Hospital of Chengdu Brain Science Institute, MOE Key Lab for Neuroinformation, School of Life Science and Technology, University of Electronic Science and Technology of China, Chengdu, 611731, China. D. Yao is with the Clinical Hospital of Chengdu Brain Science Institute, MOE Key Lab for Neuroinformation, University of Electronic Science and Technology of China, Chengdu, 611731, China, and with Research Unit of NeuroInformation 2019RU035, Chinese Academy of Medical Sciences, Chengdu, 611731, China, and with School of Electrical Engineering, Zhengzhou University, Zhengzhou, 450001, China. C. Luo is with the Clinical Hospital of Chengdu Brain Science Institute, School of Life Science and Technology, High-Field Magnetic Resonance Brain Imaging Key Laboratory of Sichuan Province, Center for Information in Medicine, University of Electronic Science and Technology of China, Chengdu, 611731, China, and with Research Unit of NeuroInformation 2019RU035, Chinese Academy of Medical Sciences, Chengdu, 611731, China. (correspondence e-mail: chengluo@uestc.edu.cn).

the diffuse activation and hypersynchrony in epilepsy may be accompanied with the altered spontaneous oscillation state. Meanwhile, the altered oscillation state may play a role on the key circuit of epileptic activity, such as the thalamocortical circuit, by regulating local activity and inter-region connections.

Human alpha rhythm, was one kind of posterior-prominent spontaneous oscillation during relaxed, eye-closed wakefulness state, generally linking with vigilance attention and consciousness. It was proposed that alpha can route the information flow via suppressing the task-irrelevant networks during cognitive operations [15, 16]. The concept of alpha inhibition was associated with the burst firing in thalamus and thalamocortical interactions [17]. Spontaneous ongoing alpha activities were also involved in pre-stimulus top-down preparation and were accounting for the cortical response to input from distant areas [18, 19]. Besides, alpha phase-synchronization has the capacity of regulating inter-regional communication to support attentional, executive and contextual function [16]. Not only that, the alterations of alpha have been considered as the hallmark of diffuse cortical-subcortical neuropathology [20, 21]. Changes of alpha rhythm was also revealed in epileptic state [22-24]. For example, slower alpha rhythm and shifted spatial topography was associated with the poorer seizure-control [24, 25]. Moreover, it was found that increased functional connectivity in low-alpha frequency band and decreased functional connectivity in high-alpha band among cortical areas coexisted and contributed to the frontal-parietal integration in IGE, which reflected the complicated physiological interdependence within alpha bands in epilepsy [26]. Therefore, alpha oscillation may provide an important role in modulations of excitatory/inhibitory balance of ongoing cortical activity to keep brain stability not only in healthy brain but epileptic brain. However, the association between the ongoing alpha oscillation and epilepsy state needs to be further elucidated. Especially, how the alpha responds for the transition from normal neuronal activity to a short-lasting generalized hyperconnectivity before GSWD remains unclear.

Based on the concurrent EEG-fMRI, some striking findings represented the regulation of the cortical activity by the dynamics of ongoing oscillations in behavioral tasks [27-29]. In this study, simultaneous EEG-fMRI was used to detect the spatiotemporal response of alpha in epileptic state. We hypothesize that there is also an existence of regulation mechanism during epileptic state arising from the ongoing alpha rhythm, and this regulation may be relevant with certain epileptic circuit. Therefore, the spatiotemporal covariation pattern between the ongoing alpha and the BOLD-based temporal dynamics as well as the spatial functional connectivity in IGE was investigated. In terms of temporal covariation, we detected the temporal representation consistency of alpha power and local BOLD fluctuations; furthermore, the effect of the temporal-varying alpha power on dynamic functional connectivity strength was analyzed. In terms of spatial covariation, the spatial network patterns in different GSWD stages were constructed, and their relationship with alpha-based network integration was also examined.

TABLE I
SUMMARY DEMOGRAPHICS OF PATIENTS AND HEALTHY CONTROLS

	HC		IGE patients		χ^2
	n=50		*n*=45		*p value*
Gender (Male/Female)	28/22		22/23		0.24
Seizure type (JME/GTCS)	-		32/13		-
	Mean	Std	Mean	Std	
Age (year)	23.9	2.1	23.5	7.1	0.382
Seizure duration (year)	-	-	8.86	6.67	-
Age at seizure onset (year)	-	-	14.64	6.65	-
Total GSWD events, *n*	-	-	2.49	2.69	-
Mean GSWD duration, *s*	-	-	4.24	5.71	-

HC: Healthy controls; Std: Standard Deviation.

II. MATERIALS AND METHODS

A. Participants

Forty-five IGE patients (23 females; mean age: 23.5 years) including 32 patients with juvenile myoclonic epilepsy (JME) and 13 patients with generalized tonic-clonic seizures (GTCS) were recruited in this study. Diagnosis and classification was made by neurologists in accordance with the International League Against Epilepsy (ILAE) guidelines [30]. Routine CT and MRI examinations were conducted and no structural abnormality was found in all epilepsy patients. Detailed clinical and seizure semiology information was showed in Supplemental Materials, sTable 1. Fifty healthy controls (HC) with no history of psychiatric or neurologic disorders participated in the study. Summary demographics of patients and healthy controls were shown in TABLE I. Written informed consent according to the Declaration of Helsinki was obtained from all participants. This study was approved by the Ethics Committee of the University of Electronic Science and Technology of China (UESTC).

B. Simultaneous EEG-fMRI acquisition and data preprocessing

Resting-state fMRI data were acquired using a 3T MRI scanner (Discovery MR750, GE) with an eight channel-phased array head coil, and a gradient-echo echo planar imaging sequences (FOV = 24 cm × 24 cm, FA = 90°, TR / TE = 2000 ms / 30 ms, matrix = 64 × 64, slice thickness / gap = 4 mm /0.4 mm). A total of 255 volumes were collected in the resting-state scan for each participant. High-resolution T1-weighted images were also acquired using a 3-D fast spoiled gradient echo (T1-3D FSPGR) sequence (FOV = 25.6 cm × 25.6 cm, FA = 9°, matrix = 256 × 256, TR / TE = 5.936 ms / 1.956 ms, slice thickness = 1 mm, no gap, 152 slices).

Simultaneous EEG were recorded by means of a MR compatible EEG cap (64-channel, Neuroscan, Charlotte, NC). Electrodes were placed according to the 10-20 standard system. Fcz was the recording reference and electrode impedances were lowered to below 10kΩ before recording. The amplifier was

settled outside the scanning room and the sampling rate was set at 5000 Hz. Synchronization between MR scanner's internal clock and the EEG recording facilitated the artifacts removal in EEG preprocessing. During the simultaneous recording, all participants were instructed to keep still and close their eyes without sleeping.

FMRI data were preprocessed using SPM12 (http://www.fil.ion.ucl.ac.uk/spm/) and NIT toolboxes (http://www.neuro.uestc.edu.cn/NIT.html) [31]. The first five volumes were discarded from all fMRI scans for the magnetization equilibrium. The remaining volumes were slice-timing corrected and spatially realigned. Individual T1 images were coregistered to the functional images, and segmented and normalized to the Montreal Neurologic Institute (MNI) space. Then, the functional images were spatial normalized based on T1 transformation matrix, resampled to $3 \times 3 \times 3$ mm^3 voxels, and spatially smoothed using a 6 mm full-width half maximum (FWHM) Gaussian kernel. Nuisance signals (12 motion parameters, linear drift signal, as well as mean white matter and cerebrospinal fluid signals) were regressed out for the fMRI data. Also, band-pass temporal filtering (0.01Hz-0.1Hz) was performed. Then, we parcellated the brain to 90 regions based on AAL atlas [32], and the averaged BOLD signal of all voxels within each region was calculated for the following network construction.

Curry 7 software (Compumedics Neuroscan) was used to correct MR gradient artifacts and the ballistocardiogram (BCG) artifacts. Before artifacts removal, we examined the EEG recording before MRI scanning, and the channels showing high impedance or electrode displacement artifacts were interpolated through a cubic spline. The gradient artifacts were corrected via template subtraction and noise cancelation [33]. The artifact template was created using a baseline-corrected sliding average of consecutive volumes. Then, the data were down-sampled to 250 Hz following the 0.5-45Hz band-pass filtering. BCG artifacts were removed using the optimal basis set (OBS) based method [34]. QRS was identified according to the electrocardiograph (ECG) channel, and the BCG artifact occurrences associated with QRS complexes were aligned in a matrix for each EEG channel, and put into a temporal principal component (PCA) analysis. The first three components describing the possible shapes, amplitudes and scales of the artifact were taken as an OBS, which was then fitted to and subtracted from each artifact occurrence. Finally, the preprocessed EEG were re-referenced to the neutral infinite reference using Reference electrode standardization technique (REST) [35].

According to the preprocessed EEG, GSWD events were identified in epilepsy patients by one neurologist, and the onset and offset time of GSWD events was marked. In order to construct the GSWD-related network, we selected GSWD epochs with the following criterion: GSWDs lasting more than 4s, with at least 20s (10TR) resting-state without discharge before and after the selected GSWDs. Finally, 28 patients each with one GSWD event were selected for the synchronization network analysis.

C. Individual alpha power estimation

For each participant, the preprocessed EEG signals (60 channels EEG without EOG and mastoid channels) was decomposed into temporal-independent components (ICs) using FastICA (http://www.cis.hut.fi/projects/ica/fastica/). Each component was characterized by a time course representing the morphology of the component over time, and by a specific spatial topography, i.e., the mixing weights. Then, the time course of ICs was cut into a series of 1-sec epochs (with 50% overlap) using a Hanning time window and submitted to fast Fourier transform (FFT). The IC showing dominant averaged power spectral in 8-14Hz and one central-posterior topography of the corresponding mixing weights was selected as the alpha-IC [36] (Supplemental Materials, sFig. 1). Then, the individual alpha frequency (IAF) was identified as a 4-Hz band centered around the alpha peak (-2 ~ +2 Hz around peak frequency) for each participant, and the average spectral power across IAF band (uV^2/Hz) for each epoch was estimated. Finally, the individual alpha power series was z-score standardized. In addition, we also used ICA to reject the residual movement-related artifacts via visual inspection. Here, the movement-related artifacts were checked referring to the individual mean frame-wise displacement (FD) values generated from fMRI preprocessing. ICs containing obvious artifacts were deleted and the EEG data were recovered based on the remaining ICs and mixing matrices.

D. Analysis of dynamic brain functional connectivity

1) Dynamic functional connectivity strength

For each subject, we calculated the whole brain dynamic functional connectivity strength (dFCS) based on sliding windows. Considering that the minimum window length was constrained by the minimum frequency of the BOLD signal (fmin), that is, the minimum window length should be not less than 1/ fmin (fmin =0.01 Hz here), here, we chose 100s (50 TR) as the sliding window length, with the sliding step width 20s (10 TR). Thus, 21 dFCS maps were obtained for each subject.

The computation of dFCS maps included: (1) The standard gray matter (GM) mask was used, and the time courses of the normalized fMRI data within GM mask were extracted; (2) The pearson correlation between each voxel pair was performed; (3) After the individual correlation matrices were Fisher-z transformed, the sum of weights of each voxel's connections was obtained to generate the whole brain FCS. Here, we used the positive threshold r=0.2 to restrict the map to eliminate the weak correlation arising from the noise, according to the significance level $P<0.001$ of the whole-brain functional connectivity at voxel level. Finally, the individual FCS maps were standardized by dividing the mean values of whole brain and further spatially smoothed (FWHM=6mm).

2) Stable phase synchronization networks in GSWD stages

Based on the phase synchronization method, dynamic large-scale brain network during GSWDs were constructed. First, according to each GSWD epoch in EEG, the fMRI segments time-locked to the GSWD onset were selected, including 10 volumes before and after GSWD, as well as the GSWD volumes. In the selected 28 GSWD epochs, most of the GSWDs

lasted 3TR and a few GSWDs lasted 2TR. In this way, the entire GSWD-related fMRI epochs were labeled TR -10 to TR -1 prior to GSWD, TR 0 to TR +1 or TR +2 during GSWD, and then the following 10TR after GSWD. Second, for a given brain region, instantaneous phase of the GSWD-related fMRI epochs was estimated using Hilbert transform, and the phase difference matrix between regions was calculated at each time point. We hypothesized that there was phase locking if their phase difference between two signals was approximately constant. Therefore, we used phase-difference derivative (PDD) to estimate the stability of the dynamic connectivity [37]. The PDD was calculated as the following:

$$\varphi_u(t) = \text{atan}(\text{Im}[\hat{A}_u(t)] / \text{Re}[\hat{A}_u(t)]) \quad (1)$$

$$PDD_{uv}(t) = \begin{cases} 1 & if \left|\frac{d\Delta\varphi_{uv}(t)}{dt}\right| \le k \\ 0 & if \left|\frac{d\Delta\varphi_{uv}(t)}{dt}\right| > k \end{cases} \quad (2)$$

Here, $\hat{A}_u(t)$ was the Hilbert transform of $A_u(t)$. $\text{Im}[\hat{A}_u(t)]$ and $\text{Re}[\hat{A}_u(t)]$ were the imaginary and real part of the signal. $\Delta\varphi_{uv}$ was the instantaneous phase difference between region *u* and *v*; $|\,|$ was the absolute value of the phase difference derivative. PDD was calculated every time point, and defined by a binary representation of dynamic phase difference between regions. That is, when phase difference derivative was small (<*k*), we assumed there was stable phase connectivity between regions, and the element of PDD was assigned value 1, otherwise the region pair was considered without stable connectivity and the element was zero. The cutoff value of *k* depended on the sample frequency, the frequency of interest and the signal to noise ratio of the data [38]. Here, we used the data-driven method and analyzed the effect of the cut-off values by means of choosing a range of *k* values (*k*=0.05, 0.1, 0.2, 0.3, 0.4). Third, the PDD matrix of a given subject in each time point, i.e. 90*90*22 binary matrix or 90*90*21 binary matrix, was submitted to a non-negative tensor factorization [39] and decomposed into 12 rank-one tensors, so as to reduce the spatiotemporal noise and spurious components of phase synchronization. The choice of component was in correspondence with the number of the typical intrinsic resting-state networks [40]. Then, the de-noised individual PDD matrix was reconstructed by first multiplying each component with its time-varying strength, and adding all the component together. Moreover, the reconstructed individual PDD matrix was normalized, that is, every element in the matrix dividing by the maximum edge value from a surrogate network. The surrogate network was generated based on the reconstructed individual PDD network of each time point, whose elements were randomized while preserving the degree distribution, and the maximum weight of the averaged surrogate network across time points was used in the normalization. Finally, the individual normalized PDD was divided into three stages: GSWD-before stage (9TR before GSWD), GSWD-onset stage (1TR or 2TR during GSWD), GSWD-after stage (9TR after GSWD). Averaged PDD matrix was calculated in each stage, and these stable phase synchronization networks were labeled as GSWD-before PDD, GSWD-onset PDD, and GSWD-after PDD. In addition, the strength of a given network node was calculated as the sum of the weights of connections with other nodes.

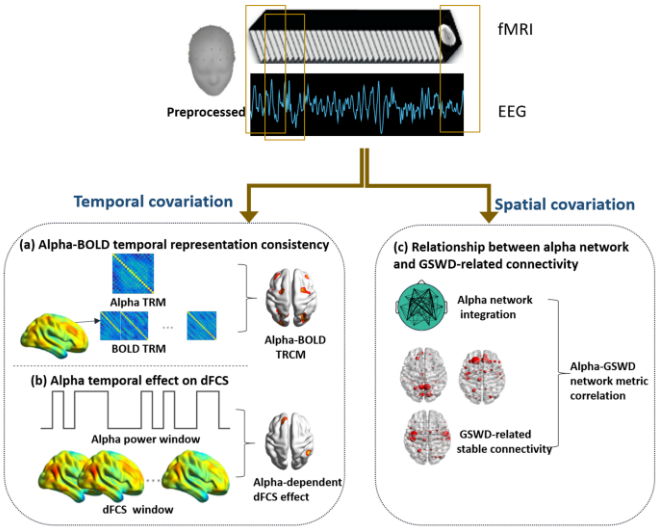

Fig. 1. Overview of the proposed framework of alpha-fMRI combination in this study: (a) Investigating the intrinsic consistency of the temporal dynamics between alpha power and BOLD fluctuations based on alpha-BOLD temporal representation correlation; (b) Examining the time-varying effect of alpha power on dFCS; (c) The fMRI-based dynamic synchronization networks during GSWDs were constructed, and the spatial covariation with alpha-based network integration was investigated.

To represent the stable synchronization network at group level, we averaged GSWD-related PDD network in different stages across all GSWD events. The significant connectivity in the group-level networks was evaluated by the histogram of the normalized PDD matrices of the three stages. The PDD values across all edges were normally distributed and the histogram was fitted by a Gaussian function. Thus, the top 1% of the most strongly connected edges were identified.

In addition, we also extracted the random epochs of the same length from HC group, i.e. 23 TR length data, and calculated the normalized PDD matrix. The significant top 1% connectivity in HC group was also identified. Moreover, the comparisons of node strength between IGE and HC group, as well as the comparisons between stages in IGE, were conducted by means of nonparametric permutation test (5000 permutations, P<0.05).

E. Alpha-fMRI combination analysis

The framework of alpha-fMRI combination was illustrated in Fig. 1, including two main parts. The first part is the temporal covariation analysis to detect the alpha-BOLD temporal representation consistency, as well as the alpha power windows effect on the global dFCS; the second part is the spatial covariation between the GSWD-related synchronization network and the alpha-based network.

1) Alpha-BOLD temporal consistency based on temporal representation correlation

Temporal representation correlation (TRC) was conducted to alpha power series and voxel-level BOLD signals to detect the intrinsic relationship of their temporal dynamics. We assumed that EEG and BOLD signals were two representations of the same neural dynamics, and may have the similar intrinsic temporal configuration. Here, the temporal representation was constructed by calculating the pearson correlation among the sliding time windows for alpha power series and voxel-level BOLD signals, respectively. The sliding time window length was 100s (50 TR), with step width 20s (10 TR), in accordance with the dFCS calculation. The correlation matrix between windows was defined as temporal representation matrix (TRM), and further, the alpha-BOLD representation correlation map (TRCM) was performed by means of calculating the correlation between alpha TRM and BOLD TRM of each voxel in the brain.

$$\begin{aligned} TRM_{Alpha} &= Corr(A_i, A_j) \qquad i, j = 1...n,\ i \neq j \\ TRM_{Bold} &= Corr(B_i, B_j) \qquad i, j = 1...n,\ i \neq j \\ TRCM &= Corr(TRM_{Alpha}, TRM_{Bold}) \end{aligned} \tag{3}$$

Here, A_i and A_j was the time course of alpha power in time window *i* and *j*, and B_i and B_j was the time course of voxel-level BOLD signal in time window *i* and *j*. To obtain the within-group TRCM, one sample t-test was conducted for IGE and HC group, respectively. Two sample t-test was also performed to examine the difference of TRCM between IGE and HC group.

In addition, we selected a series of sliding windows when calculating TRMs to test the effect of time widows and the stability of the result, including 50TR window length with 10TR step width, 50TR window length with 5TR step width, and 40TR window length with 20TR step width.

2) Temporal-varying effect of alpha power on dFCS

In order to examine the effect of alpha power fluctuation on dFCS, the same length time windows as fMRI-based dFCS were applied to alpha power series. All the windows were grouped into the higher power windows and the lower power windows according to the comparison between the mean power within window and mean power of the whole series. Thus, the individual dFCS maps were divided into two groups based on the alpha power windows, and the averaged dFCS map in each group was obtained. In this way, each subject had two alpha-dependent dFCS maps, i.e., high alpha window dependent dFCS maps, and low alpha window dependent dFCS maps.

Further, two-way repeated measures ANOVA (2 group * 2 power_window) was performed for alpha-dependent dFCS maps to detect the group effect, the alpha window effect, and the interactive effect.

3) Spatial covariation between PDD network and alpha network integration

According to the comparison results of stable PDD node strength between IGE and HC, we selected the nodes which represented significant difference between GSWD stages and HC group, and calculated the pearson correlation between the node strength and the network metric of scalp alpha. Here, the network metric of the scalp alpha was the characteristic path length of the network [41], which was one measurement of functional integration of the network. The scalp alpha network was constructed using imaginary coherence between electrodes, and this method was thought to be insensitive to false connectivity arising from volume conduction [42]. After the EEG epochs of GSWD stages in IGE, as well as the EEG random epochs in HC subjects were extracted, imaginary coherence between electrodes in individual alpha band for all subjects was calculated. Then, functional integration of scalp alpha network was estimated by the characteristic path length. The smaller length of paths represented much stronger integration of the whole network. The calculation of imaginary coherence and the characteristic path length of network was as follows:

$$ImgC(f) = \left| img\left[\frac{|C_{ij}(f)|}{C_{ii}(f)C_{jj}(f)} \right] \right| \tag{4}$$

$$L = \frac{1}{n} \sum_{i \in N} L_i = \frac{1}{n} \sum_{i \in N} \frac{\sum_{j \in N, j \neq i} d_{ij}}{n-1} \tag{5}$$

Here, *ImgC*(*f*) is the absolute imaginary coherence between electrode *i* and *j*, under frequency *f*. In this study, we calculated the averaged imaginary coherence in IAF for each subject. Then, the characteristic path length of the coherence network was calculated as the averaged shortest path length of each node, and *n* is the number of network nodes, d_{ij} is shortest path length between electrode *i* and *j*.

III. Result

A. Alpha-BOLD temporal representation correlation map

Alpha-BOLD TRCM was illustrated in Fig. 2. Generally, dominant positive correlation was found ($P<0.001$), which indicated that alpha and BOLD signals, as two representations of the same neural activity, had intrinsic relationship in terms of their temporal dynamics. In HC group, alpha-BOLD TRCM was mainly located at thalamus, occipital, precuneus and part of frontal cortex, while in IGE group, much more distributed and enhanced alpha-BOLD TRCM was found, including the frontal, parietal, temporal, occipital areas, as well as subcortical regions, i.e., thalamus and caudate. In between-group comparison, significant increased TRCM was found in IGE, mainly including the pre- and post-central area, frontal area, thalamus and caudate. Regions with significant alpha-BOLD TRCM in IGE, HC group and between-group comparison were demonstrated in Supplemental Materials, sTable 2. In addition, consistent significant alpha-BOLD TRCM was found in the conditions of different window length and step width, and the effect of time window was slight, but with much weak significance in the condition of shorter window length and larger step width (Supplemental Materials, sFig. 2).

B. Temporal-varying effect of alpha power on dFCS

The results of ANOVAs about the alpha-dependent dFCS was shown in Fig. 3, including the group effect, alpha power window effect and their interactive effect (Supplemental Materials, sTable 3). The main group effect was found in bilateral precuneus. DFCS in thalamus and some

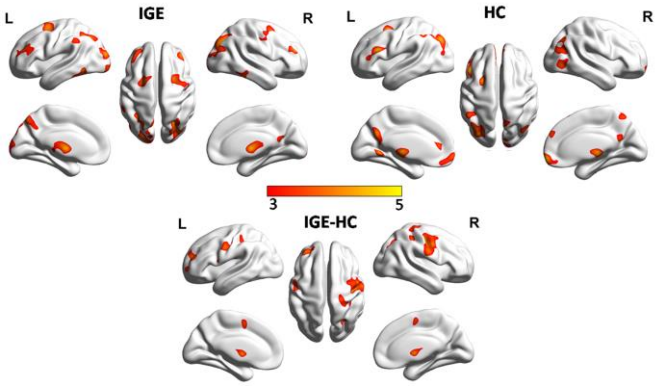

Fig. 2. Regions showing significant alpha-BOLD temporal representation correlation in IGE, HC group and between-group comparison (P<0.001).

cortical regions such as parietal_inf, frontal_sup and frontal_sup_medial cortex showed dependence on the level of alpha power windows. In addition, the interactive effect between group and alpha power was mainly reflected in frontal area and caudate. These regions, including precuneus, parietal_inf, frontal_sup and frontal_sup_medial, were widely involved in DMN template, which was obtained through group spatial ICA (Supplemental Materials, sFig. 3). Therefore, for HC, there was dominant inhibition effect of alpha power on dFCS, that is, the increased alpha power was accompanied with decreased dFCS in frontal regions and caudate. While in IGE, the higher alpha power along with the higher dFCS in caudate, thalamus and some DMN regions, may indicate the temporal regulation of alpha power to the functional connectivity in epileptic brain.

C. Stable GSWD-related synchronization network

We constructed the PDD networks in different GSWD-related stages. In order to test the effect of cutoff *k* value, we calculated the PDD matrix in the condition of a range of *k* values, and computed the averaged PDD strength of 90 regions across subjects (Supplemental Materials, sFig. 4). Significant correlation among PDD strength with different *k* values (mean correlation coefficient > 0.7, P<0.0001) reflected that there was slight effect of cutoff *k* value on the synchronization connectivity. Here, we demonstrated the PDD networks based on a threshold *k* of 0.2. GSWD-before network, GSWD-onset network, and GSWD-after network of the group level were shown in Fig. 4 (a)-(c). In GSWD-before network, precuneus was the main hub node. The connectivity within parietal-occipital area was dominant, and a few of connections between the precuneus and frontal, as well as the temporal areas existed. In GSWD-onset network, the hub node transferred to frontal_mid area, and dominant connectivity among frontal areas was represented. Furthermore, in GSWD-after network, the motor-related regions near central sulcus, including pre-central, post-central area and rolandic_oper area, have become the new hub regions, and strong connectivity among them was found. In HC group, a widely distributed network throughout the brain was shown, and interhemispheric and long-range anterior-posterior connectivity constituted the stable phase synchronization network (Fig. 4 (d)).

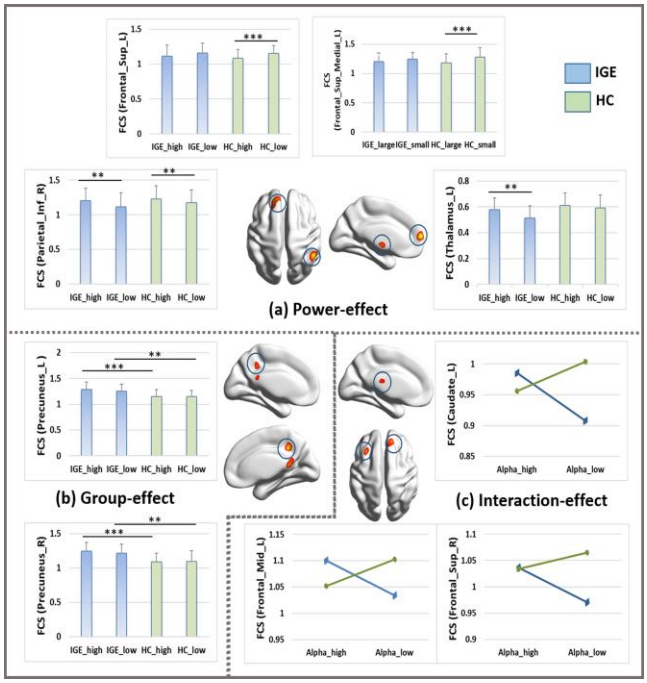

Fig. 3. Regions showing significant group effect, power window effect and interactive effect of dFCS (P<0.001). The bar maps present the post-hoc differences in the regions highlighted using blue circle. In the bar maps, _high denotes high alpha power window, and _low denotes low alpha power window, **P<0.005, ***P<0.001. The green bars and lines denote HC group, while the blue bars and lines denote IGE group.

Moreover, between-group comparisons in terms of the node strength in PDD network were calculated based on nonparametric permutation test (P<0.05) (Fig. 4 (e)-(g)). In GSWD-before stage, enhanced stable connectivity was revealed in parietal_inf and precuneus, while reduced stable connectivity appeared in motor-related regions near central sulcus, and subcortical regions involving putamen and pallidum. In GSWD-onset stage, more subcortical regions showed increased stable connectivity. While in GSWD-after stage, there was increased stable connectivity in precuneus and parietal area, as well as some temporal regions. In addition, much higher network connectivity strength in GSWD-onset network was shown comparing to the other two stages (Supplemental Materials, sFig. 5). Between-stages comparisons of the PDD node strength in IGE were also conducted using nonparametric test. More frontal and subcortical areas showed higher connectivity strength in GSWD-onset stage (Fig. 4 (h)-(i)). The detailed regions with significant difference of PDD node strength between IGE and HC, as well as between GSWD stages were shown in Supplemental Materials, sTable 4-5.

D. Relationship between PDD network and alpha network integration

Here, we investigated the relationship between PDD network and alpha-based network (Fig. 5). Comparing to HC group, IGE group represented much lower network integration, that is the longer network characteristic path length in GSWD-onset stage. Moreover, alpha network metric showed negative correlation with epilepsy seizure frequency in IGE, which demonstrated the

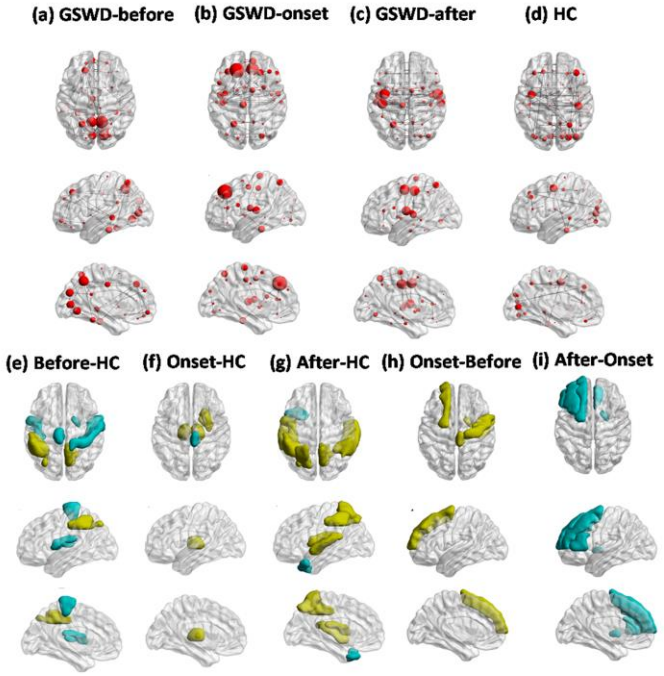

Fig. 4. Stable phase synchronization connectivity of IGE and HC. (a)-(c) PDD network patterns in GSWD-before, GSWD-onset and GSWD-after stages. In the network configuration, the size of the node denoted the connectivity strength of this node. (d) PDD network pattern of HC group. (e)-(g) Between-group comparisons in terms of the PDD node strength between GSWD stages and HC group, and the regions showing significant difference were revealed. (h)-(i): Between-stage comparisons in terms of the PDD node strength. The yellow regions denote increased connectivity strength, and the blue regions denote decreased connectivity strength.

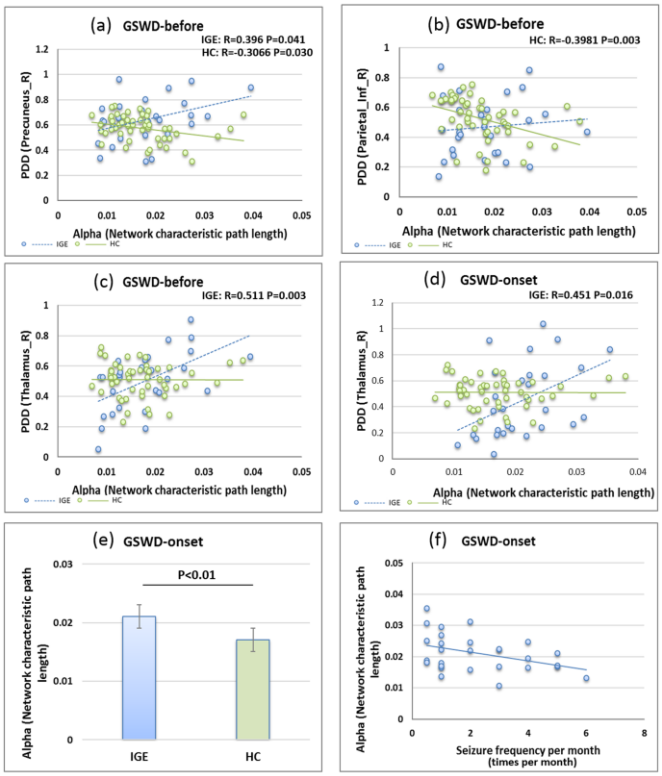

Fig. 5. (a)-(d) Relationship between PDD network strength and the characteristic path length of the scalp alpha network. (e) Comparing to HC, IGE group showed significant larger characteristic path length of alpha network in GSWD-onset stage. (f) In GSWD-onset stage, negative relationship was found between the characteristic path length of alpha network and the seizure frequency per month in patients with IGE.

patients with disturbed alpha network integration often had better seizure-control.

In HC, PDD network strength in parietal areas including parietal_inf and precuneus demonstrated negative correlation with the characteristic path length of alpha network, that is, these regions showed stronger PDD connectivity along with the higher alpha network integration. However, this negative correlation disappeared and tended to be positive in precuneus in IGE group before GSWDs. In addition, thalamus also showed positive correlation between PDD network strength and alpha network metric in GSWD-before and GSWD-onset stage. The results meant that there was hyperconnectivity in precuneus and thalamus accompanied with lower alpha network integration, which may indicate the spatial regulation of alpha oscillation to the hyperconnectivity in terms of the decreased inter-region communication in epilepsy. In addition, we also detected the alpha-power and its relationship with PDD network during GSWD stages. Comparing to HC, alpha power was increased in GSWD-before stage. Moreover, this increase of alpha power was accompanied with the enhancement of PDD network strength in precuneus and thalamus.

IV. Discussion

This study investigated the association between two representations of the neurophysiology in brain: the scalp alpha rhythm and BOLD fluctuation. We hypothesized that the ongoing alpha can spatiotemporally act on the distributed activation and altered functional connectivity in epileptic brain. The results demonstrated that the alpha-BOLD temporal covariation was stronger and more distributed in IGE than HC. Moreover, temporal-varying alpha power showed inhibition effect on dynamic functional connectivity in frontal cortex in HC, while IGE represented the higher alpha power along with the higher dFCS in subcortical and some DMN regions. Furthermore, we constructed the stable synchronized networks in different GSWD-related stages. The hyperconnectivity in prominent nodes (precuneus, thalamus) was accompanied with the decreased alpha-based network integration. These results indicated the spatiotemporal regulation of alpha by means of increased power and decreased coherence communication in epilepsy state, and clarified that thalamus and DMN regions (precuneus, frontal area) were key nodes in epileptic circuit associated with alpha regulation.

A. Temporal covariation of alpha with local BOLD activity and dFCS

In this study, we used a novel method to detect the consistency between EEG temporal representation and BOLD temporal representation. Previous studies have reported the spatial involvement of alpha-related BOLD response, such as the thalamus, frontal, parietal and occipital areas [43-45]. One recent study proposed that the dynamics of the alpha power and BOLD signals were two different representations of the same underlying neural activity, and their relationship ensued from variations in the strengths of corticothalamic and intrathalamic

feedback [46]. The current study demonstrated that the covariation of intrinsic temporal dynamics between alpha rhythm and BOLD fluctuations was mainly located at thalamus, occipital and DMN regions in HC. The temporal representation correlation method made full use of the similarity of temporal structure of the same neural activity underlying alpha and BOLD fluctuation, and would provide a new perspective for EEG-fMRI fusion. Especially, this method would avoid the variation of hemodynamic response functions (HRF), which occurred across different regions and individuals [47]. Moreover, enhanced and widespread alpha-BOLD covariation was found in epilepsy, mainly locating at the frontal, pre- and post-central area, and subcortical areas. These regions were also frequently reported as GSWDs-related regions [48-50], which may imply the close links between alpha response and GSWDs in epilepsy. In previous study, both alpha frequency and alpha dynamics were changed due to epilepsy activity [22, 51]. The enhanced covariation of alpha and BOLD activity may reflect the regulation mechanism of alpha to the local epilepsy activity. Moreover, thalamus was considered to be the generator and modulator of EEG alpha rhythm [17, 52]. Therefore, the involvement of thalamus with increased consistency of alpha-BOLD temporal representation may imply the dependence of alpha temporal regulation on the thalamus in epilepsy brain [53].

Besides, the temporal-varying alpha power effect on the dFCS was also demonstrated in the current study. Subcortical regions and some frontal cortices involved in DMN were significantly dependent on the dynamics of alpha power. Previous studies have frequently shown that the frontal areas were related to alpha rhythm, and the connectivity among these regions and thalamus was relevant to the alpha power dynamic [46, 54]. Moreover, temporal regulation of oscillations was suggested imposing excitability windows to route the information and to facilitate inter-regional interactions [55]. Therefore, the power window effect of alpha on the functional connectivity may suggested one kind of temporal regulation arising from alpha, which was realized through the higher alpha windows suppressing the dFCS in certain regions. However, in IGE group, much higher alpha power existed along with the increased dFCS in frontal, parietal areas, thalamus and caudate, which reflected the close link between alpha power dynamics and the hyperconnectivity in DMN and subcortical areas in IGE.

B. Stable GSWD-related synchronization network in IGE

In this study, stable functional connectivity in epochs including GSWD events was constructed based on phase synchronization method. Although BOLD signals were much more slowly fluctuations due to the low haemodynamic response, phase synchronization has shown valuable performance about the dynamic functional brain networks in previous fMRI studies [37, 40, 56]. Our findings provided the stable functional networks regarding to GSWD-before, GSWD-onset, as well as GSWD-after stages. In GSWD-before stage, a stable network mainly located in the parietal and occipital areas was revealed, with the highly connected hub node, precuneus. As one key part of DMN, precuneus has been widely reported involved in epilepsy-related network [57-59]. Activity changes in precuneus has been documented for several seconds before GSWD [10], and fMRI study using dynamic causal modeling suggested that activity in precuneus gated GSWD in the thalamocortical network [60]. One previous EEG study also showed precuneus was the regions with the maximal outdegree during spike onset stage [61]. Therefore, the increased stable connectivity in precuneus before GSWDs indicated the important role of the precuneus on initiating and sustaining GSWDs.

In GSWD-onset stage, dominant connectivity among frontal and parietal areas was represented, and the middle frontal gyrus was the prominent hub in this network. Frontal-central predominance of GSWD was always found in EEG recordings [62], and abnormal frontal involvement has also been consistently demonstrated in various neuroimaging researches [63-66]. One previous study directly examining the fMRI time course in absence seizures showed the increase of BOLD response involving widespread bilateral frontal and temporal cortex during and after seizure onset [67]. In the other hand, the striatum was also suggested involving in the regulation of epileptic discharge, and enhanced functional connectivity in striatum was accompanied with the increasing of discharges [68]. Moreover, the striatum regulated GSWD by contributing to the thalamocortical circuit [69]. Therefore, the widely distributed connectivity in frontal, as well as the increased connectivity in thalamus and striatum during GSWD-onset stage supported the involvement of striato–thalamo–frontal network in GSWD onset and propagation.

In GSWD-after stage, one inter-hemispheric network among sensorimotor areas was observed. BOLD activation in sensorimotor areas was associated with GSWDs and the enhanced EEG network variation in IGE [70]. Hyperconnectivity in motor system was proposed to be associated with the epilepsy syndrome, such as the myoclonic jerks [26, 71]. The prominent network involving sensorimotor area may imply the consequence of the thalamo-frontal interaction after GSWD onset.

C. Spatial covariation of PDD network and alpha network

Abnormality in alpha band activity was proposed to represent the unbalance of the excitatory/inhibitory state of ongoing neural activity, such as the alpha frequency alteration in epilepsy [17, 72]. Besides the alpha power, decreased alpha network integration was also found in GSWD-onset stage in the current study. There were numerous findings demonstrated that alpha oscillations served to route information by local inhibition function, while alpha phase-synchronization among regions had the capacity of regulating inter-regional interaction to support cognitive functions [73, 74]. Occipital, parietal, as well as frontal regions were reportedly associated with scalp alpha, and the connectivity among these regions could facilitate the long-range communications in brain [54]. In this study, increased functional connectivity in post-DMN regions (parietal_inf area, precuneus) was related to the enhanced integration of alpha network, which demonstrated the role of alpha network in the functional integration in healthy brain. While in IGE, disturbed alpha network was found in GSWD-

onset stage, and accompanied with the increased functional connectivity in precuneus and thalamus. These results may imply the spatial regulation of alpha, that is, alpha try to suppress the hyperconnectivity during GSWDs via the decreased alpha-network integration. Moreover, this regulation may depend on the involvement of thalamus and DMN regions.

D. Pathophysiological interpretation and clinical potentials

This study provided new perspective about the link between EEG spontaneous oscillation and fMRI functional connectivity from both temporal and spatial dimensions. Alpha oscillations were associated with thalamic burst firings, and the reciprocal thalamocortical circuit was crucial in the generation of alpha oscillations [75]. The dynamics of alpha rhythm posited an active role in the balance of excitatory/inhibitory, resulting to the desynchronization hypothesis (function of routing by inhibition), as well as the synchronization hypothesis (function of long-range communication) [16, 55]. Here, the covariation between the enhanced alpha power and the hyperconnectivity involving the thalamus, caudate, and some DMN regions reflected that alpha played a role in the epilepsy circuit. Further, based on dynamic phase synchronization, key regions and network patterns during different GSWD stages were demonstrated. These patterns proposed that the hyperconnectivity of precuneus may be the physiological initiator of discharges, and the interaction of thalamo-frontal circuit facilitated the propagation of GSWDs [10]. The results supported the cortical triggering and thalamocortical theory for generalized spike-wave discharges, and may provide supplemental information for clinical practice. Moreover, alpha rhythm demonstrated increased power and decreased coherence before and during GSWD onset stage. These accompanying changes of alpha and functional connectivity may imply abnormal representation of the abrupt change of epilepsy brain. However, we tend to assume that the ongoing alpha oscillation stood out to regulate or suppress the sudden epileptic activity by means of the increased power and destroyed coherence communication across brain. Also, the relationship between alpha metric and averaged seizure frequency of patients gave evidence that this destroyed alpha network integration was helpful for the seizure-control. In addition, the patients with IGE were more vulnerable during wake-up time [76], which may imply the failure of alpha regulation because of the changed consciousness state and excitatory/inhibitory unbalance. Therefore, this study provided hint to regulate the deep brain nuclei via modulating perceptually relevant brain oscillations, i.e. alpha rhythm, in a frequency-specific manner, and may be of practical clinical importance in terms of seizure prediction and non-invasive intervention using transcranial current stimulation or magnetic stimulation in epilepsy.

E. Limitations and methodological considerations

There are several methodological issues and limitations in this study. The first concern might be the temporal correspondence of the rapidly fluctuated alpha and the delayed fMRI due to the hemodynamic response. Here, we assumed that alpha and BOLD fluctuation were two representations of the brain activity and potential links between their dynamics existed. Therefore, we adopted a symmetric EEG-fMRI fusion method, and segmented alpha and BOLD-based images into dynamic time windows of the same length to detect the relationship between them, which may be helpful for avoiding the canonical problem of HRF variation. However, the great difference in the temporal courses between EEG and BOLD signals was non-negligible. In traditional EEG-informed fMRI analysis, EEG features were often convolved with the HRF to match fMRI activities. Here, in the analysis of alpha-BOLD temporal representation correlation, the correlations among alpha windows will be slightly influenced when each window convolving with one specific function, i.e., HRF. Moreover, in the analysis of alpha-dependent dFCS, we selected long-enough time windows (100s), and the effect arising from the delay of the hemodynamic response (about 5s-8s) on the window-to-window correspondence would be weakened. Besides, we re-conducted the temporal-varying alpha-dependent dFCS analysis, where alpha power series was convolved with the canonical HRF in advance, and most consistent results were demonstrated (Supplemental Materials, sFig. 6). Second, the selection of the dynamic windows seemed arbitrary in the study, although we considered the minimum frequency of the BOLD signals. Therefore, we re-tested the alpha-BOLD TRCM and alpha-dependent dFCS via changing the time window length, and stable results were showed. Because we focused on the relationship between two modalities using the same time windows, the window effect may be weakened. Third, the decision of alpha power using ICA may be another concern. The procedure of the independent component selection sounds complex comparing to the traditional method, i.e., single or multi-channel averaging of the occipital channels. However, considering the individual difference, as well as the alteration of alpha frequency and spatial distribution in epilepsy patients, we chose this data-driven method without priori choices. Finally, no causal links were constructed between functional connectivity and alpha rhythm was the main limitation in this study. Future work using causal model was urgent to determine the pathophysiological mechanisms and alpha regulation to the thalamocortical circuit in epilepsy.

V. CONCLUSION

Our findings provided links between the scalp alpha rhythm and BOLD activity, as well as the stable synchronization network constructed during GSWDs. Increased and more distributed alpha-BOLD temporal consistency was found in IGE, and the hyperconnectivity in prominent nodes (thalamus, frontal and parietal area) was associated with the increased alpha power and disturbed alpha-based network integration. These results may imply the temporal and spatial regulation of alpha via thalamus-default mode circuit when facing the distributed activation and hyperconnectivity in epilepsy and may be of practical clinical importance in terms of seizure prediction and non-invasive interventions.

REFERENCE

[1] M. P. Richardson, "Large scale brain models of epilepsy: dynamics meets connectomics," Journal of Neurology Neurosurgery and Psychiatry, vol. 83, pp. 1238-1248, Dec 2012.

[2] Z. Q. Zhang, W. Liao, H. F. Chen, D. Mantini, J. R. Ding, Q. Xu, et al., "Altered functional-structural coupling of large-scale brain networks in idiopathic generalized epilepsy," Brain, vol. 134, pp. 2912-2928, Oct 2011.

[3] Z. G. Wang, S. Lariviere, Q. Xu, R. V. de Wael, S. J. Hong, Z. Y. Wang, et al., "Community-informed connectomics of the thalamocortical system in generalized epilepsy," Neurology, vol. 93, pp. E1112-E1122, Sep 10 2019.

[4] H. Blumenfeld, "From molecules to networks: Cortical/subcortical interactions in the pathophysiology of idiopathic generalized epilepsy," Epilepsia, vol. 44, pp. 7-15, 2003.

[5] C. P. Panayiotopoulos, T. Obeid, and A. R. Tahan, "Juvenile Myoclonic Epilepsy - a 5-Year Prospective-Study," Epilepsia, vol. 35, pp. 285-296, Mar-Apr 1994.

[6] H. Blumenfeld, "Cellular and network mechanisms of spike-wave seizures," Epilepsia, vol. 46, pp. 21-33, 2005.

[7] P. Gloor, "Hans Berger on Electroencephalography," American Journal of Eeg Technology, vol. 9, pp. 1-8, 1969.

[8] J. T. Paz, J. M. Deniau, and S. Charpier, "Rhythmic bursting in the cortico-subthalamo-pallidal network during spontaneous genetically determined spike and wave discharges," Journal of Neuroscience, vol. 25, pp. 2092-2101, Feb 23 2005.

[9] F. Amor, S. Baillet, V. Navarro, C. Adam, J. Martinerie, and M. L. Van Quyen, "Cortical local and long-range synchronization interplay in human absence seizure initiation," Neuroimage, vol. 45, pp. 950-962, Apr 15 2009.

[10] F. Moeller, H. R. Siebner, S. Wolff, H. Muhle, R. Boor, O. Granert, et al., "Changes in activity of striato-thalamo-cortical network precede generalized spike wave discharges," Neuroimage, vol. 39, pp. 1839-49, Feb 15 2008.

[11] E. R. John, "From synchronous neuronal discharges to subjective awareness?," vol. 150, pp. 143-593, 2005.

[12] G. Buzsaki and A. Draguhn, "Neuronal oscillations in cortical networks," Science, vol. 304, pp. 1926-1929, Jun 25 2004.

[13] W. Klimesch, "EEG alpha and theta oscillations reflect cognitive and memory performance: a review and analysis," Brain Research Reviews, vol. 29, pp. 169-195, Apr 1999.

[14] B. Clemens, "Pathological theta oscillations in idiopathic generalised epilepsy," Clinical Neurophysiology, vol. 115, pp. 1436-1441, Jun 2004.

[15] W. Klimesch, P. Sauseng, and S. Hanslmayr, "EEG alpha oscillations: The inhibition-timing hypothesis," Brain Research Reviews, vol. 53, pp. 63-88, Jan 2007.

[16] S. Palva and J. M. Palva, "New vistas for alpha-frequency band oscillations," Trends Neurosci, vol. 30, pp. 150-8, Apr 2007.

[17] S. W. Hughes and V. Crunelli, "Thalamic mechanisms of EEG alpha rhythms and their pathological implications," Neuroscientist, vol. 11, pp. 357-372, Aug 2005.

[18] I. B. H. Samuel, C. Wang, Z. Hu, and M. Ding, "The frequency of alpha oscillations: Task-dependent modulation and its functional significance," Neuroimage, vol. 183, pp. 897-906, Dec 2018.

[19] K. Usami, G. W. Milsap, A. Korzeniewska, M. J. Collard, Y. Wang, R. P. Lesser, et al., "Cortical Responses to Input From Distant Areas are Modulated by Local Spontaneous Alpha/Beta Oscillations," Cereb Cortex, vol. 29, pp. 777-787, Feb 1 2019.

[20] L. B. Hinkley, S. Vinogradov, A. G. Guggisberg, M. Fisher, A. M. Findlay, and S. S. Nagarajan, "Clinical symptoms and alpha band resting-state functional connectivity imaging in patients with schizophrenia: implications for novel approaches to treatment," Biol Psychiatry, vol. 70, pp. 1134-42, Dec 15 2011.

[21] K. Johnston, L. Ma, L. Schaeffer, and S. Everling, "Alpha Oscillations Modulate Preparatory Activity in Marmoset Area 8Ad," J Neurosci, vol. 39, pp. 1855-1866, Mar 6 2019.

[22] P. G. Larsson and H. Kostov, "Lower frequency variability in the alpha activity in EEG among patients with epilepsy," Clin Neurophysiol, vol. 116, pp. 2701-6, Nov 2005.

[23] J. Pyrzowski, M. Sieminski, A. Sarnowska, J. Jedrzejczak, and W. M. Nyka, "Interval analysis of interictal EEG: pathology of the alpha rhythm in focal epilepsy," Scientific Reports, vol. 5, Nov 10 2015.

[24] A. Stoller, "Slowing of the alpha-rhythm of the electroencephalogram and its association with mental deterioration and epilepsy," J Ment Sci, vol. 95, pp. 972-84, Oct 1949.

[25] E. Abela, A. D. Pawley, C. Tangwiriyasakul, S. N. Yaakub, F. A. Chowdhury, R. D. C. Elwes, et al., "Slower alpha rhythm associates with poorer seizure control in epilepsy," Annals of Clinical and Translational Neurology, vol. 6, pp. 333-343, Feb 2019.

[26] B. Clemens, S. Puskas, M. Besenyei, T. Spisak, G. Opposits, K. Hollody, et al., "Neurophysiology of juvenile myoclonic epilepsy: EEG-based network and graph analysis of the interictal and immediate preictal states," Epilepsy Research, vol. 106, pp. 357-369, Oct 2013.

[27] R. Becker, M. Reinacher, F. Freyer, A. Villringer, and P. Ritter, "How Ongoing Neuronal Oscillations Account for Evoked fMRI Variability," Journal of Neuroscience, vol. 31, pp. 11016-11027, Jul 27 2011.

[28] R. Scheeringa, A. Mazaheri, I. Bojak, D. G. Norris, and A. Kleinschmidt, "Modulation of Visually Evoked Cortical fMRI Responses by Phase of Ongoing Occipital Alpha Oscillations," Journal of Neuroscience, vol. 31, pp. 3813-3820, Mar 9 2011.

[29] K. Uludag and A. Roebroeck, "General overview on the merits of multimodal neuroimaging data fusion," Neuroimage, vol. 102, pp. 3-10, Nov 15 2014.

[30] J. Engel, "A proposed diagnostic scheme for people with epileptic seizures and with epilepsy: Report of the ILAE Task Force on Classification and Terminology," Epilepsia, vol. 42, pp. 796-803, Jun 2001.

[31] L. Dong, C. Luo, X. B. Liu, S. S. Jiang, F. L. Li, H. S. Feng, et al., "Neuroscience Information Toolbox: An Open Source Toolbox for EEG-fMRI Multimodal Fusion Analysis," Frontiers in Neuroinformatics, vol. 12, Aug 24 2018.

[32] N. Tzourio-Mazoyer, B. Landeau, D. Papathanassiou, F. Crivello, O. Etard, N. Delcroix, et al., "Automated anatomical labeling of activations in SPM using a macroscopic anatomical parcellation of the MNI MRI single-subject brain," Neuroimage, vol. 15, pp. 273-289, Jan 2002.

[33] P. J. Allen, O. Josephs, and R. Turner, "A method for removing imaging artifact from continuous EEG recorded during functional MRI," Neuroimage, vol. 12, pp. 230-239, Aug 2000.

[34] R. K. Niazy, C. F. Beckmann, G. D. Iannetti, J. M. Brady, and S. M. Smith, "Removal of FMRI environment artifacts from EEG data using optimal basis sets," Neuroimage, vol. 28, pp. 720-737, Nov 15 2005.

[35] D. Yao, "A method to standardize a reference of scalp EEG recordings to a point at infinity," Physiological Measurement, vol. 22, pp. 693-711, 2001.

[36] R. Scheeringa, K. M. Petersson, A. Kleinschmidt, O. Jensen, and M. C. Bastiaansen, "EEG alpha power modulation of fMRI resting-state connectivity," Brain Connect, vol. 2, pp. 254-64, 2012.

[37] P. Tewarie, B. A. E. Hunt, G. C. O'Neill, A. Byrne, K. Aquino, M. Bauer, et al., "Relationships Between Neuronal Oscillatory Amplitude and Dynamic Functional Connectivity," Cereb Cortex, vol. 29, pp. 2668-2681, Jun 1 2019.

[38] F. Babiloni, D. Mattia, C. Babiloni, L. Astolfi, S. Salinari, A. Basilisco, et al., "Multimodal integration of EEG, MEG and fMRI data for the solution of the neuroimage puzzle," Magn Reson Imaging, vol. 22, pp. 1471-6, Dec 2004.

[39] L. Gauvin, A. Panisson, and C. Cattuto, "Detecting the Community Structure and Activity Patterns of Temporal Networks: A Non-Negative Tensor Factorization Approach," Plos One, vol. 9, Jan 31 2014.

[40] C. Tangwiriyasakul, S. Perani, M. Centeno, S. N. Yaakub, E. Abela, D. W. Carmichael, et al., "Dynamic brain network states in human generalized spike-wave discharges," Brain, vol. 141, pp. 2981-2994, Oct 1 2018.

[41] M. Rubinov and O. Sporns, "Complex network measures of brain connectivity: uses and interpretations," Neuroimage, vol. 52, pp. 1059-69, Sep 2010.

[42] G. Nolte, O. Bai, L. Wheaton, Z. Mari, S. Vorbach, and M. Hallett, "Identifying true brain interaction from EEG data using the imaginary part of coherency," Clinical Neurophysiology, vol. 115, pp. 2292-2307, Oct 2004.

[43] R. I. Goldman, J. M. Stern, J. Engel, and M. S. Cohen, "Simultaneous EEG and fMRI of the alpha rhythm," Neuroreport, vol. 13, pp. 2487-2492, Dec 20 2002.

[44] Z. Liu, J. A. de Zwart, B. Yao, P. van Gelderen, L. W. Kuo, and J. H. Duyn, "Finding thalamic BOLD correlates to posterior alpha EEG," Neuroimage, vol. 63, pp. 1060-9, Nov 15 2012.

[45] M. Moosmann, P. Ritter, I. Krastel, A. Brink, S. Thees, F. Blankenburg, et al., "Correlates of alpha rhythm in functional magnetic resonance

imaging and near infrared spectroscopy," Neuroimage, vol. 20, pp. 145-58, Sep 2003.

[46] J. C. Pang and P. A. Robinson, "Neural mechanisms of the EEG alpha-BOLD anticorrelation," Neuroimage, vol. 181, pp. 461-470, Nov 1 2018.

[47] G. K. Aguirre, E. Zarahn, and M. D'Esposito, "The variability of human, BOLD hemodynamic responses," Neuroimage, vol. 8, pp. 360-9, Nov 1998.

[48] Y. Aghakhani, A. P. Bagshaw, C. G. Benar, C. Hawco, F. Andermann, F. Dubeau, et al., "fMRI activation during spike and wave discharges in idiopathic generalized epilepsy," Brain, vol. 127, pp. 1127-1144, May 2004.

[49] Z. Q. Zhang, W. Liao, Z. G. Wang, Q. Xu, F. Yang, D. Mantini, et al., "Epileptic discharges specifically affect intrinsic connectivity networks during absence seizures," Journal of the Neurological Sciences, vol. 336, pp. 138-145, Jan 15 2014.

[50] J. Gotman, C. Grova, A. Bagshaw, E. Kobayashi, Y. Aghakhani, and F. Dubeau, "Generalized epileptic discharges show thalamocortical activation and suspension of the default state of the brain," Proc Natl Acad Sci U S A, vol. 102, pp. 15236-40, Oct 18 2005.

[51] V. M. Uritskii, V. B. Slezin, E. A. Korsakova, S. K. Khorshev, and N. I. Muzalevskaya, "Fractal diagnostics of disturbances in the dynamics of alpha-rhythm in epilepsy patients," Biofizika, vol. 44, pp. 1109-1114, Nov-Dec 1999.

[52] M. Schreckenberger, C. Lange-Asschenfeld, M. Lochmann, K. Mann, T. Siessmeier, H. G. Buchholz, et al., "The thalamus as the generator and modulator of EEG alpha rhythm: a combined PET/EEG study with lorazepam challenge in humans," Neuroimage, vol. 22, pp. 637-644, Jun 2004.

[53] M. L. Lorincz, K. A. Kekesi, G. Juhasz, V. Crunelli, and S. W. Hughes, "Temporal framing of thalamic relay-mode firing by phasic inhibition during the alpha rhythm," Neuron, vol. 63, pp. 683-96, Sep 10 2009.

[54] H. Laufs, A. Kleinschmidt, A. Beyerle, E. Eger, A. Salek-Haddadi, C. Preibisch, et al., "EEG-correlated fMRI of human alpha activity," Neuroimage, vol. 19, pp. 1463-76, Aug 2003.

[55] S. Palva and J. M. Palva, "Functional roles of alpha-band phase synchronization in local and large-scale cortical networks," Front Psychol, vol. 2, p. 204, 2011.

[56] E. Glerean, J. Salmi, J. M. Lahnakoski, I. P. Jaaskelainen, and M. Sams, "Functional magnetic resonance imaging phase synchronization as a measure of dynamic functional connectivity," Brain Connect, vol. 2, pp. 91-101, 2012.

[57] L. Dong, C. Luo, Y. Zhu, C. Hou, S. Jiang, P. Wang, et al., "Complex discharge-affecting networks in juvenile myoclonic epilepsy: A simultaneous EEG-fMRI study," Hum Brain Mapp, vol. 37, pp. 3515-29, Oct 2016.

[58] J. N. Guo, R. Kim, Y. Chen, M. Negishi, S. Jhun, S. Weiss, et al., "Impaired consciousness in patients with absence seizures investigated by functional MRI, EEG, and behavioural measures: a cross-sectional study," The Lancet Neurology, vol. 15, pp. 1336-1345, 2016.

[59] X. Jia, Y. Xie, D. Dong, H. Pei, S. Jiang, S. Ma, et al., "Reconfiguration of dynamic large-scale brain network functional connectivity in generalized tonic-clonic seizures," Hum Brain Mapp, vol. 41, pp. 67-79, Jan 2020.

[60] A. E. Vaudano, H. Laufs, S. J. Kiebel, D. W. Carmichael, K. Hamandi, M. Guye, et al., "Causal hierarchy within the thalamo-cortical network in spike and wave discharges," PLoS One, vol. 4, p. e6475, Aug 3 2009.

[61] C. Lee, S. M. Kim, Y. J. Jung, C. H. Im, D. W. Kim, and K. Y. Jung, "Causal influence of epileptic network during spike-and-wave discharge in juvenile myoclonic epilepsy," Epilepsy Res, vol. 108, pp. 257-66, Feb 2014.

[62] H. Luders, R. P. Lesser, D. S. Dinner, and H. H. Morris, 3rd, "Generalized epilepsies: a review," Cleve Clin Q, vol. 51, pp. 205-26, Summer 1984.

[63] F. Benuzzi, L. Mirandola, M. Pugnaghi, V. Farinelli, C. A. Tassinari, G. Capovilla, et al., "Increased cortical BOLD signal anticipates generalized spike and wave discharges in adolescents and adults with idiopathic generalized epilepsies," Epilepsia, vol. 53, pp. 622-630, Apr 2012.

[64] S. S. Jiang, X. K. Li, Z. L. Li, X. B. Chang, Y. Chen, Y. Huang, et al., "Cerebello-cerebral connectivity in idiopathic generalized epilepsy," European Radiology, vol. 30, pp. 3924-3933, Jul 2020.

[65] S. S. Jiang, C. Luo, Y. Huang, Z. L. Li, Y. Chen, X. Li, et al., "Altered static and dynamic spontaneous neural activity in drug-naïve and drug-receiving benign childhood epilepsy with centrotemporal spikes.," Frontiers in Human Neuroscience, 2020.

[66] J. H. Kim, S. I. Suh, S. Y. Park, W. K. Seo, I. Koh, S. B. Koh, et al., "Microstructural white matter abnormality and frontal cognitive dysfunctions in juvenile myoclonic epilepsy," Epilepsia, vol. 53, pp. 1371-8, Aug 2012.

[67] X. Bai, M. Vestal, R. Berman, M. Negishi, M. Spann, C. Vega, et al., "Dynamic time course of typical childhood absence seizures: EEG, behavior, and functional magnetic resonance imaging," J Neurosci, vol. 30, pp. 5884-93, Apr 28 2010.

[68] C. Luo, Q. F. Li, Y. Xia, X. Lei, K. Q. Xue, Z. P. Yao, et al., "Resting state basal ganglia network in idiopathic generalized epilepsy," Human Brain Mapping, vol. 33, pp. 1279-1294, Jun 2012.

[69] C. Deransart, V. Riban, B. T. Le, C. Marescaux, and A. Depaulis, "Dopamine in the striatum modulates seizures in a genetic model of absence epilepsy in the rat," Neuroscience, vol. 100, pp. 335-344, 2000.

[70] Y. Qin, S. Jiang, Q. Zhang, L. Dong, X. Jia, H. He, et al., "BOLD-fMRI activity informed by network variation of scalp EEG in juvenile myoclonic epilepsy," Neuroimage Clin, vol. 22, p. 101759, Mar 12 2019.

[71] C. Vollmar, J. O'Muircheartaigh, G. J. Barker, M. R. Symms, P. Thompson, V. Kumari, et al., "Motor system hyperconnectivity in juvenile myoclonic epilepsy: a cognitive functional magnetic resonance imaging study," Brain, vol. 134, pp. 1710-1719, Jun 2011.

[72] P. G. Larsson, O. Eeg-Olofsson, and G. Lantz, "Alpha frequency estimation in patients with epilepsy," Clin EEG Neurosci, vol. 43, pp. 97-104, Apr 2012.

[73] O. Jensen, B. Gips, T. O. Bergmann, and M. Bonnefond, "Temporal coding organized by coupled alpha and gamma oscillations prioritize visual processing," Trends in Neurosciences, vol. 37, pp. 357-369, Jul 2014.

[74] W. Klimesch, "Alpha-band oscillations, attention, and controlled access to stored information," Trends in Cognitive Sciences, vol. 16, pp. 606-617, Dec 2012.

[75] M. A. Nicolelis and E. E. Fanselow, "Thalamocortical optimization of tactile processing according to behavioral state," Nat Neurosci, vol. 5, pp. 517-23, Jun 2002.

[76] R. A. B. Badawy, R. A. L. Macdonell, G. D. Jackson, and S. F. Berkovic, "Why do seizures in generalized epilepsy often occur in the morning?," Neurology, vol. 73, pp. 218-222, 2009.